# The benefit of combining curcumin, bromelain and harpagophytum to reduce inflammation in osteoarthritic synovial cells

Sybille Brochard, Julien Pontin, Benoit Bernay, Karim Boumediene, Thierry Conrozier, Catherine Baugé

BMC Complementary Medicine and Therapies

RESEARCH

Open Access

# The benefit of combining curcumin, bromelain and harpagophytum to reduce inflammation in osteoarthritic synovial cells

Sybille Brochard[1], Julien Pontin[2], Benoit Bernay[2], Karim Boumediene[1], Thierry Conrozier[3] and Catherine Baugé[1*]

## Abstract

**Background:** Osteoarthritis (OA) is the most common form of arthritis, affecting millions of people worldwide and characterised by joint pain and inflammation. It is a complex disease involving inflammatory factors and affecting the whole joint, including the synovial membrane. Since drug combination is widely used to treat chronic inflammatory diseases, a similar strategy of designing plant-derived natural products to reduce inflammation in OA joints may be of interest. In this study, we characterised the response of OA synovial cells to lipopolysaccharide (LPS) and investigated the biological action of the combination of curcumin, bromelain and harpagophytum in this original in vitro model of osteoarthritis.

**Methods:** Firstly, human synovial cells from OA patients were stimulated with LPS and proteomic analysis was performed. Bioinformatics analyses were performed using Cytoscape App and SkeletalVis databases. Additionally, cells were treated with curcumin, bromelain and harpagophytum alone or with the three vegetal compounds together. The gene expression involved in inflammation, pain or catabolism was determined by RT-PCR. The release of the encoded proteins by these genes and of prostaglandin E2 (PGE2) were also assayed by ELISA.

**Results:** Proteomic analysis demonstrated that LPS induces the expression of numerous proteins involved in the OA process in human OA synovial cells. In particular, it stimulates inflammation through the production of pro-inflammatory cytokines (Interleukin-6, IL-6), catabolism through an increase of metalloproteases (MMP-1, MMP-3, MMP-13), and the production of pain-mediating neurotrophins (Nerve Growth Factor, NGF). These increases were observed in terms of mRNA levels and protein release. LPS also increases the amount of PGE2, another inflammation and pain mediator. At the doses tested, vegetal extracts had little effect: only curcumin slightly counteracted the effects of LPS on NGF and MMP-13 mRNA, and PGE2, IL-6 and MMP-13 release. In contrast, the combination of curcumin with bromelain and harpagophytum reversed lots of effects of LPS in human OA synovial cells. It significantly reduced the gene expression and/or the release of proteins involved in catabolism (MMP-3 and -13), inflammation (IL-6) and pain (PGE2 and NGF).

**Conclusion:** We have shown that the stimulation of human OA synovial cells with LPS can induce protein changes similar to inflamed OA synovial tissues. In addition, using this model, we demonstrated that the combination of three

*Correspondence: catherine.bauge@unicaen.fr
[1] EA7451 BioConnect, Université de Caen Normandie, UNICAEN, 14032 Caen, France
Full list of author information is available at the end of the article

vegetal compounds, namely curcumin, bromelain and harpagophytum, have anti-inflammatory and anti-catabolic effects in synovial cells and may thus reduce OA progression and related pain.

## Introduction

Osteoarthritis (OA) is a debilitating and painful disease characterised by inflammation of the synovial membrane and the progressive destruction of articular cartilage [1, 2]. It is one of the top 10 causes of physical disability [3]. However, its aetiology and pathogenesis are still not fully understood. Long considered a simple degenerative cartilage disease, OA is now described as a global joint disease [4]. To date, no treatment has been able to reverse OA progression.

Although OA is not classified as an inflammatory disease, many reports suggest that inflammation could be a major driver of OA development. In fact, elevated joint inflammation has been correlated with progression of the disease [5]. Therefore, although OA pathogenesis remains unclear, inflammation is widely regarded as an extremely important factor for the progression of this disease [2, 6–8] and pain severity [9–11].

Synovitis, i.e. the inflammation of synovial tissues, is common in OA [12] and is mediated, in part, by fibroblast-like synoviocytes (FLS). These cells play an important role in OA inflammation and joint destruction, primarily by secreting a wide range of proinflammatory mediators, such as IL-6 and prostaglandin E2 (PGE2) [12], which leads the release of neurotrophins such as NGF, leading to pain during OA. They also secrete various type of proteases, including matrix metalloproteinases (MMPs) and the A Disintegrin and Metalloproteinase with Thrombospondin Motifs family (or enzymes) (ADAMTS) [13], thus promoting the degradation of extracellular cell matrix (ECM) and further aggravating the progression of OA. Therefore, alleviating synovial inflammation may prevent the onset or minimise the progression of OA and symptoms [2, 14–16]. Conventional anti-inflammatory drugs are nonsteroidal anti-inflammatory drugs (NSAIDs) [17]. However, these entail several side effects and drug interactions, including the risk of gastrointestinal, cardiovascular and kidney problems. The use of natural compounds may be a relevant alternative.

Herbal medicine has been used since ancient times for healing purposes and is still used today. Curcumin (CUR), which is extracted from the rhizome of *Curcuma longa* L., is one of the most ancient medicinal herbs and is widely used in human health due to its various therapeutic features, such as anti-inflammatory, antioxidant, anticancer and antimicrobial effects [18]. In patients with OA, oral administration of curcumin improves the clinical manifestation of the disease [19–22], improves quality of life and enables a decrease in the consumption of NSAIDs [23]. This beneficial effect of curcumin is associated with its ability to reduce OA inflammation in cells, animal models and human studies [24, 25]. The action of curcumin may be reinforced by combining with other natural compounds [18, 26].

The purpose of the study was to investigate the effects of the combination of curcumin (CUR), bromelain (BRO) — a food obtained from pineapple which has analgesic properties [27] — and harpagophytum (HAR) — a traditional remedy for articular diseases [28] — on inflammation in an original in vitro model of osteoarthritis, using human synovial cells treated with lipopolysaccharide (LPS).

## Material and methods

### Reagents

Lipopolysaccharide (LPS) from *E.Coli* (Sigma Aldrich, Saint Louis, USA) was dissolved in phosphate buffer saline with no Calcium or Magnesium (DPBS, Lonza, Basel, Switzerland) in order to reach a concentration of 1 mg/ml, and was used once a final concentration of 1 µg/ml was attained. Curcumin (Turmeric extract granules, 95% curcuminoids, Natural, St Sylvain d'Anjou, France) was resuspended in dimethyl sulfoxide (DMSO, Dutscher, Bernolsheim, France). For the harpagophytum (*Harpagophytum procumbens*, Biosearch Life, Granada, Spain) and bromelain (Bromelain 2500 GDU, Cambridge Commodities Ltd., Ely, UK) extracts, the suspension was carried out in DPBS. The concentration of curcumin used was 13 µM (stock solution 130 mM), bromelain 14.7 µg/ml (stock solution 147 mg/ml) and harpagophytum 36 µg/ml (360 mg/ml).

### Culture cells and treatments

Human synoviocytes were recovered from the synovial membrane of six patients undergoing hip replacement surgery (mean age = 75 years). The cells were released by enzymatic digestion of the synovial membrane with collagenase type I (2 mg/ml, 12 h; ThermoFisher, Waltham, USA). The cells were cultured in Dulbecco's Modified Eagle Medium high glucose with glutamine and sodium pyruvate (DMEM, Dutscher), supplemented with 10% Foetal Bovine Serum (FBS, Dutscher) and penicillin-streptomycin (Lonza), then incubated at 37 °C in a humid atmosphere containing 5% $CO_2$.

To achieve the desired number of cells, passages were performed. The cells were rinsed with DPBS, then detached with 0.05% trypsin (ThermoFisher). The cells were recovered in a culture medium and seeded at approximately 7500 cells/cm$^2$. The absence of mycoplasmas was checked by PCR.

The cells were processed at the confluence stage. Treatments were diluted in a new culture medium to the desired concentration. Each molecule was tested alone or in the presence of LPS. The three molecules were also tested together in order to see the effects of the combination of these three extracts, in the presence and absence of LPS.

#### Protein extraction

Cells were lysed and protein extracted using Radio Immuno Precipitation Assay (RIPA) Buffer (50 mM Tris-HCl pH 7.5; 1% Igepal CA-630; 150 mM NaCl; 1 mM EGTA; 1 mM NaF; 0.25% Na-deoxycholate; Distilled water), and supplemented with a protease inhibitor (Leupeptin 1 mg/m; Phenyl methyl sulfonyl fluoride 200 m; pepstatin A 1 mg/ml) and a phosphatase inhibitor (sodium orthovanadate 200 mM) as previously described [29].

#### Proteomic experiment

Five µg of each protein extract was prepared using a modified Gel-aided Sample Preparation protocol [30]. Samples were digested with trypsin/Lys-C overnight at 37 °C. For nano-LC fragmentation, protein or peptide samples were first desalted and concentrated onto a µC18 Omix (Agilent) before analysis.

The chromatography step was performed on a nanoElute (Bruker Daltonics) ultra-high pressure nano-flow chromatography system. Approximatively 200 ng of each peptide sample was concentrated onto a C18 PepMap 100 (5 mm × 300 µm i.d.) precolumn (Thermo Scientific) and separated at 50 °C onto a reversed phase ReproSil column (25 cm × 75 µm i.d.) packed with 1.6 µm C18 coated porous silica beads (IonOpticks). Mobile phases consisted of 0.1% formic acid, 99.9% water (v/v) (A) and 0.1% formic acid in 99.9% ACN (v/v) (B). The nanoflow rate was set at 400 nl/min, and the gradient profile was as follows: from 2 to 15% B within 60 min, followed by an increase to 25% B within 30 min and further to 37% within 10 min, followed by a washing step at 95% B and re-equilibration.

Mass spectrometry (MS) experiments were carried out on an TIMS-TOF pro mass spectrometer (Bruker Daltonics) with a modified nano electrospray ion source (CaptiveSpray, Bruker Daltonics). The system was calibrated each week and mass precision was better than 1 ppm. A 1600 spray voltage with a capillary temperature of 180 °C was typically employed for ionising. MS spectra were acquired in the positive mode in the mass range of 100 to 1700 m/z. In the experiments described here, the mass spectrometer was operated in Parallel Accumulation Serial Fragmentation (PASEF) mode with the exclusion of single charged peptides [31]. A number of 10 PASEF MS/MS scans were performed for 1.25 s from a charge range of 2–5.

Before the post-processing, the samples were analysed using Preview software (Protein Metrics) in order to estimate the quality of the tryptic digestion and predict the post-translational modifications present. The result, below, is used for the 'bank research/identification' part. The fragmentation pattern was used to determine the sequence of the peptide. Database searching was performed using the Peaks X+ software. A UniProt *Homo sapiens* database (October 2020) was used. The variable modifications allowed were as follows: N-terminal acetylation, methionine oxidation, Deamidation (NQ), Methylation (KR) and Carbamylation. In addition, C-Propionamide was set as the fixed modification. 'Trypsin' was selected as Specific. Mass accuracy was set to 30 ppm and 0.05 Da for the MS and MS/MS modes respectively. Data were filtered according to a false discovery rate (FDR) of 0.5% and protein redundancy was eliminated on the basis of proteins being evidenced by the same set or subset of peptides.

#### Identification of differentially expressed proteins

To quantify the relative levels of protein abundance between different groups, samples were analysed using the label-free quantification feature of PEAKS X+ software [32]. Feature detection was separately performed on each sample by the expectation-maximisation algorithm. The features of the same peptide from all replicates of each sample were aligned through the retention time alignment algorithms. Mass error tolerance was set at 30 ppm, Ion Mobility Tolerance (1/k0) at 0.07 and retention time tolerance at 10 min. Normalisation factors of the samples were obtained by the total ion current (TIC) of each sample. Quantification of the protein abundance level was calculated using the sum area of the top three unique peptides. A 1.5-fold increase in relative abundance and a significance of $\geq$5 using ANOVA as the significance method were used to determine those enriched proteins.

#### Enrichment analysis and comparison with datasets related to skeletal biology

The heatmap technique was performed with a Spearman clustering method using the ComplexHeatmap R package.

Enrichments in the molecular processes, cellular processes and pathways (KEGG and Reactome) were performed using the ClueGo App from the Cytoscape software. Network specificity was set to medium; the GO tree interval was set between 2 and 4. Clusters were performed using a selection set to a minimum of three genes in addition to 4% of genes. Enrichments were performed using a Bonferroni step-down method.

Additionally, differentially expressed proteins were compared to existing gene expression datasets related to skeletal biology using the SkeletalVis application (http://skeletalvis.ncl.ac.uk/skeletal/, [33]). Proteins encoded by genes associated with osteoarthritis joint damage in animals were also identified using OATargets databases [34].

#### RNA extraction and RT-PCR

RNA was extracted from the cell layer using the RNeasy mini kit (Qiagen, Hilden, Germany) in accordance with the supplier's protocol. Then, DNase treatment and reverse transcription were carried out using the DNase I kit (Sigma Aldrich) and the reverse transcriptase M-MLV (Invitrogen, Carlsbad, USA) as previously described [35]. Next, cDNA was amplified by real-time PCR using a PCR master Mix (Power SYBR Green, Applied biosystems, Courtaboeuf, France) and read on the Step One Plus Real Time PCR system (Applied Biosystems) with the following primers: RPL13A Forward: 5′-GAGGTATGCTGCCCCACAAA-3′ and Reversed: 5′-GTGGGATGCCGTCAAACAC-3′; NGF Forward: 5′-AGCGCAGCGAGTTTTGG-3′ and Reversed: 5′-AGAAAGCTGCTCCCTTGGTA-3′; IL-6 Forward: 5′-CACACAGACAGCCACTCACC-3′ and Reversed: 5′-TTTCACCAGGCAAGTCTCCT-3′; MMP-1 Forward: 5′-GAAGCTGCTTACGAATTTGCCG-3′ and Reversed: 5′-CCAAAGGAGCTGTAGATGTCCT-3′; MMP-3 Forward: 5′-TAAAGACAGGCACTT TTGGCGC-3′ and Reversed: 5′-TTGGGTATCCAGCTCGTACCTC-3′; MMP-13 Forward: 5′-AAGGAGCATGGCGACTTCT-3′ and Reversed: 5′-TGGCCCAGGAGGAAAAGC-3′. The relative mRNA level was calculated using the $2^{-\Delta\Delta CT}$ method. RPL13a was used as the invariant housekeeping gene. The decision to opt for this gene was based on our previous experience in the field [29, 35, 36].

#### Elisa

PGE2 and MMP released into conditioned media were quantified using a commercially available enzyme immunoassay kit (R&D Biosystem) as previously described [29]. For IL-6, we proceeded in the same way but using the Human beta-NGF ELISA Kit and the Human IL-6 ELISA kit (Sigma Aldrich). The immunoassays were all carried out in accordance with the manufacturer's protocol. Absorbance was determined at 450 nm with a wavelength correction set at 540 nm using the Multiskan GO spectrophotometer (Thermo Scientific).

#### Statistical analyses

All results are expressed as the mean value of three or four patients (biological replicates) $\pm$ the standard error of the mean (SEM). Statistical analyses were carried out on the GraphPad prism 8 software. After checking the normal distribution of samples, two-way ANOVA tests were used for multiple comparisons. In significant cases, Tukey's multiple comparisons test for matched samples was performed as a post-hoc analysis. *P*-values < 0.05 were considered significant.

## Results

#### Stimulation of human OA synovial cells with LPS, an efficient OA model in vitro

Lipopolysaccharide (LPS) has recently been considered a stimulus which is able to trigger inflammation and OA onset, and is used to model the inflammatory component of OA. Therefore, we planned to test the effects of curcumin, harpagophytum and bromelain in human OA synovial cells stimulated with LPS. Before doing so, we wanted to validate the model and its ability to model OA inflammation. So, we conducted a proteomic analysis to define the differentially expressed proteins from among unstimulated OA synovial cells and LPS-stimulated OA synovial cells. Two thousand nine hundred seventeen proteins were identified in the control group, and 3011 in the LPS treated-group. Among them, 106 proteins were differentially expressed between the two groups (Peaks Sign > 5, Fold-change > 1.5, Fig. 1 and Table 1). More precisely, 66 proteins (i.e. 62%) were significantly downregulated by LPS, and 40 (i.e. 38%) were upregulated by LPS. ClueGo analysis revealed that these differentially expressed proteins are mainly involved in the biological processes of oxidative stress-induced cell death (45%, *p*-value < 0.01) and in the molecular processes of intramolecular oxidoreductase activity (25%, *p*-value < 0.01) and collagen binding (12.5%, *p*-value < 0.01) (Fig. 2, Tables 2 and 3). Furthermore, KEGG pathway enrichment (Fig. 3A, Table 4) showed the presence of proteins involved in protein digestion and absorption, fructose and mannose metabolism, and antigen processing and presentation (33% for each, *p*-value < 0.01). Enrichment using Reactome (Fig. 3B, Table 5) also showed the presence of proteins involved in the assembly of collagen fibrils and other multimeric structures (24%, *p*-value < 0.05).

The signature comparison of the proteomic profiles of the control group and the LPS-stimulated synovial cells using the SkeletalVis database, which allowed us

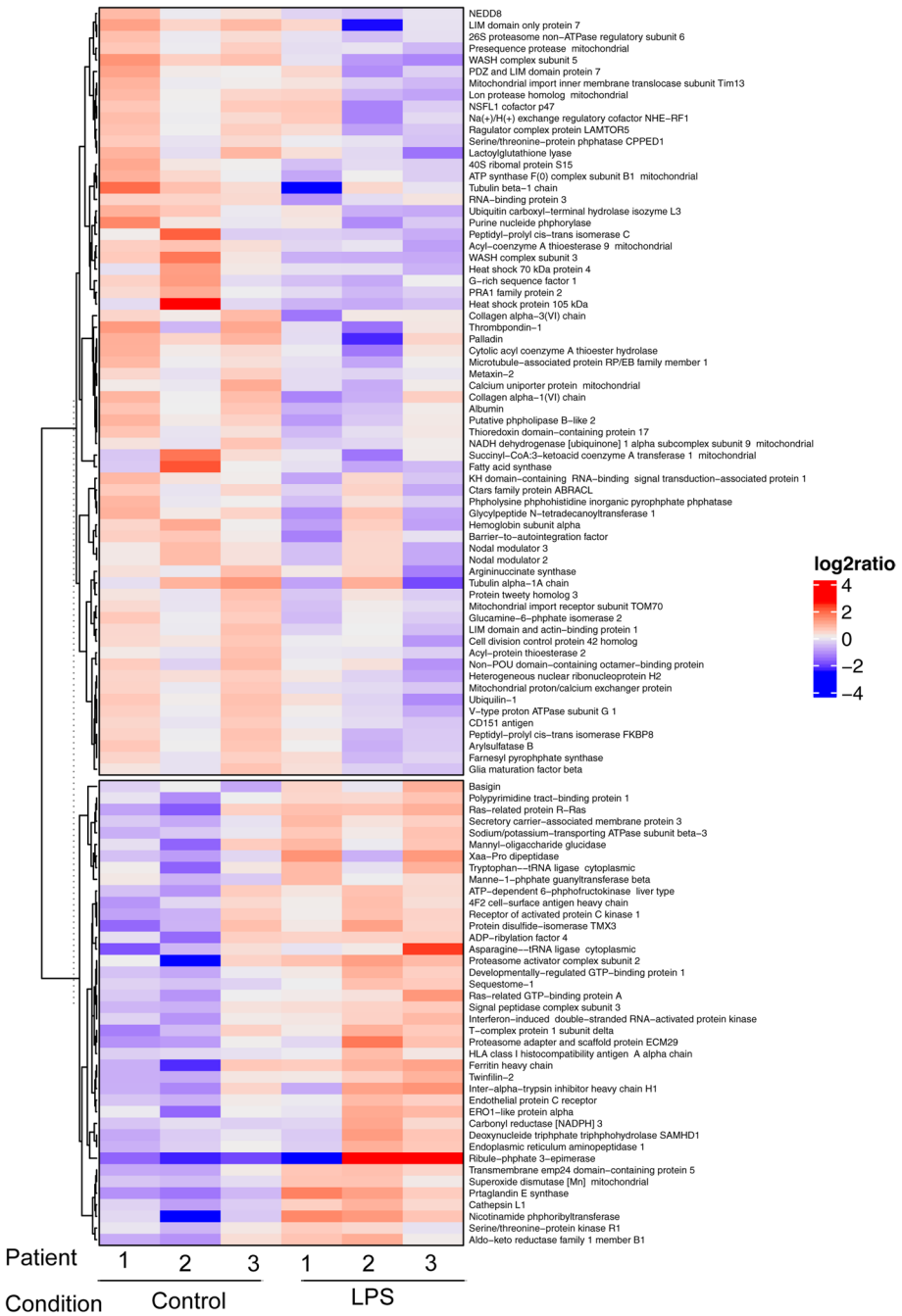


**Fig. 1** Heatmap showing differentially expressed proteins by LPS in human synovial cells. Human synovial cells from three different patients were treated with LPS (1 µg/ml) for 48 h. At the end of the experiments, proteins were extracted and proteomic analysis was performed. Differentially expressed proteins from among the control group and the LPS group is shown ($n = 3$)

to explore skeletal biology-related expression datasets [33], suggested that deregulated proteins were encoded by genes which are also differentially expressed in several other OA models (suppl. Data 1), namely 'Synovial cells from inflammatory and normal areas of osteoarthritis synovial membrane' (signed Jaccard index (sig) = 0.015; z score = 5.08) and observed in 'Rat model of surgically induced knee osteoarthritis' (signed

**Table 1** List of deregulated proteins in LPS-stimulated synovial cells

| Accession | Group Profile (Ratio) | Gene names (primary) | Description | OA associated | human OA DEG | induced OA DEG | OA gene interaction | skeletal phenotype |
|---|---|---|---|---|---|---|---|---|
| ***Proteins down-regulated by LPS*** | | | | | | | | |
| Q92598 | 0.23 | HSPH1 | Heat shock protein 105 kDa | false | 2 | 8 | 14 | false |
| P49327 | 0.25 | FASN | Fatty acid synthase | false | 3 | 7 | 17 | false |
| Q9Y3C0 | 0.26 | WASHC3 | WASH complex subunit 3 | false | 1 | 1 | 3 | false |
| Q9H4B7 | 0.32 | TUBB1 | Tubulin beta-1 chain | false | 5 | 1 | 3 | false |
| P45877 | 0.36 | PPIC | Peptidyl-prolyl cis-trans isomerase C | false | 8 | 9 | 0 | false |
| Q12768 | 0.43 | WASHC5 | WASH complex subunit 5 | false | 0 | 0 | 2 | false |
| P07996 | 0.45 | THBS1 | Thrombpondin-1 | true | 4 | 2 | 19 | true |
| Q8WWI1 | 0.45 | LMO7 | LIM domain only protein 7 | false | 3 | 5 | 7 | false |
| Q8WX93 | 0.47 | PALLD | Palladin | false | 3 | 2 | 5 | false |
| Q8NHP8 | 0.48 | PLBD2 | Putative phpholipase B-like 2 | false | 0 | 0 | 2 | false |
| Q8NE86 | 0.49 | MCU | Calcium uniporter protein mitochondrial | false | 0 | 0 | 0 | false |
| O60831 | 0.51 | PRAF2 | PRA1 family protein 2 | false | 1 | 3 | 0 | false |
| Q9UMX0 | 0.52 | UBQLN1 | Ubiquilin-1 | false | 1 | 1 | 15 | false |
| Q9NR12 | 0.52 | PDLIM7 | PDZ and LIM domain protein 7 | false | 5 | 3 | 7 | false |
| O00154 | 0.52 | ACOT7 | Cytolic acyl coenzyme A thioester hydrolase | false | 0 | 3 | 1 | false |
| Q9Y305 | 0.53 | ACOT9 | Acyl-coenzyme A thioesterase 9 mitochondrial | false | 0 | 4 | 6 | false |
| Q71U36 | 0.53 | TUBA1A | Tubulin alpha-1A chain | false | 1 | 1 | 31 | false |
| P15374 | 0.53 | UCHL3 | Ubiquitin carboxyl-terminal hydrolase isozyme L3 | false | 0 | 7 | 5 | false |
| Q04760 | 0.53 | GLO1 | Lactoylglutathione lyase | false | 0 | 3 | 3 | true |
| P30419 | 0.53 | NMT1 | Glycylpeptide N-tetradecanoyltransferase 1 | false | 1 | 1 | 4 | false |
| P55809 | 0.54 | OXCT1 | Succinyl-CoA:3-ketoacid coenzyme A transferase 1 mitochondrial | false | 2 | 4 | 3 | false |
| O43504 | 0.55 | LAMTOR5 | Ragulator complex protein LAMTOR5 | false | 0 | 1 | 4 | false |
| P62841 | 0.55 | RPS15 | 40S ribomal protein S15 | false | 1 | 5 | 9 | false |
| P36776 | 0.55 | LONP1 | Lon protease homolog mitochondrial | false | 4 | 3 | 7 | false |
| Q12849 | 0.55 | GRSF1 | G-rich sequence factor 1 | false | 0 | 1 | 2 | false |
| Q5JRX3 | 0.55 | PITRM1 | Presequence protease mitochondrial | false | 2 | 3 | 2 | false |
| Q8TDQ7 | 0.55 | GNPDA2 | Glucamine-6-phphate isomerase 2 | false | 0 | 1 | 1 | false |
| P34932 | 0.56 | HSPA4 | Heat shock 70 kDa protein 4 | false | 0 | 2 | 39 | false |
| Q15691 | 0.56 | MAPRE1 | Microtubule-associated protein RP/EB family member 1 | false | 0 | 0 | 13 | false |
| P24539 | 0.56 | ATP5PB | ATP synthase F(0) complex subunit B1 mitochondrial | false | 0 | 0 | 6 | false |
| P00491 | 0.56 | PNP | Purine nucleide phphorylase | false | 6 | 3 | 1 | false |
| P69905 | 0.56 | HBA1; HBA2 | Hemoglobin subunit alpha | false | 7 | 0 | 3 | false |
| Q15008 | 0.57 | PSMD6 | 26S proteasome non-ATPase regulatory subunit 6 | false | 0 | 5 | 4 | false |
| P02768 | 0.57 | ALB | Albumin | false | 2 | 0 | 9 | false |
| Q9UHB6 | 0.57 | LIMA1 | LIM domain and actin-binding protein 1 | false | 2 | 4 | 9 | true |

**Table 1** (continued)

| Accession | Group Profile (Ratio) | Gene names (primary) | Description | OA associated | human OA DEG | induced OA DEG | OA gene interaction | skeletal phenotype |
|---|---|---|---|---|---|---|---|---|
| Q15843 | 0.57 | NEDD8 | NEDD8 | false | 0 | 3 | 9 | false |
| P15848 | 0.58 | ARSB | Arylsulfatase B | false | 3 | 6 | 1 | true |
| O95202 | 0.58 | LETM1 | Mitochondrial proton/calcium exchanger protein | false | 0 | 2 | 3 | false |
| P12109 | 0.59 | COL6A1 | Collagen alpha-1(VI) chain | true | 6 | 12 | 9 | false |
| Q9UNZ2 | 0.59 | NSFL1C | NSFL1 cofactor p47 | false | 0 | 1 | 8 | false |
| Q9Y5L4 | 0.59 | TIMM13 | Mitochondrial import inner membrane translocase subunit Tim13 | false | 0 | 3 | 3 | false |
| P55795 | 0.61 | HNRNPH2 | Heterogeneous nuclear ribonucleoprotein H2 | false | 0 | 2 | 5 | true |
| Q9H008 | 0.61 | LHPP | Phpholysine phphohistidine inorganic pyrophphate phphatase | false | 4 | 5 | 0 | false |
| P12111 | 0.62 | COL6A3 | Collagen alpha-3(VI) chain | false | 6 | 16 | 2 | true |
| O14745 | 0.62 | SLC9A3R1 | Na(+)/H(+) exchange regulatory cofactor NHE-RF1 | false | 1 | 4 | 11 | true |
| P98179 | 0.62 | RBM3 | RNA-binding protein 3 | false | 1 | 1 | 5 | false |
| Q14318 | 0.62 | FKBP8 | Peptidyl-prolyl cis-trans isomerase FKBP8 | false | 1 | 2 | 10 | true |
| O94826 | 0.62 | TOMM70 | Mitochondrial import receptor subunit TOM70 | false | 0 | 2 | 4 | false |
| P48509 | 0.62 | CD151 | CD151 antigen | false | 0 | 1 | 0 | false |
| O75348 | 0.62 | ATP6V1G1 | V-type proton ATPase subunit G 1 | false | 1 | 2 | 0 | false |
| P60953 | 0.63 | CDC42 | Cell division control protein 42 homolog | true | 0 | 0 | 19 | true |
| Q9BRA2 | 0.63 | TXNDC17 | Thioredoxin domain-containing protein 17 | false | 1 | 1 | 0 | false |
| Q9BRF8 | 0.63 | CPPED1 | Serine/threonine-protein phphatase CPPED1 | false | 2 | 0 | 0 | false |
| Q07666 | 0.64 | KHDRBS1 | KH domain-containing RNA-binding signal transduction-associated protein 1 | false | 0 | 2 | 16 | true |
| Q16795 | 0.64 | NDUFA9 | NADH dehydrogenase [ubiquinone] 1 alpha subcomplex subunit 9 mitochondrial | false | 0 | 2 | 6 | false |
| O75431 | 0.64 | MTX2 | Metaxin-2 | false | 0 | 1 | 0 | false |
| Q9C0H2 | 0.64 | TTYH3 | Protein tweety homolog 3 | false | 1 | 4 | 0 | false |
| Q5JPE7 | 0.64 | NOMO2 | Nodal modulator 2 | false | 0 | 0 | 1 | false |
| P69849 | 0.64 | NOMO3 | Nodal modulator 3 | false | 0 | 0 | 1 | false |
| P00966 | 0.65 | ASS1 | Argininuccinate synthase | false | 4 | 2 | 4 | false |
| O75531 | 0.65 | BANF1 | Barrier-to-autointegration factor | false | 0 | 2 | 2 | false |
| O95372 | 0.65 | LYPLA2 | Acyl-protein thioesterase 2 | false | 0 | 0 | 1 | false |
| Q9P1F3 | 0.65 | ABRACL | Ctars family protein ABRACL | false | 3 | 2 | 0 | false |
| Q15233 | 0.66 | NONO | Non-POU domain-containing octamer-binding protein | false | 0 | 2 | 16 | false |
| P14324 | 0.66 | FDPS | Farnesyl pyrophphate synthase | false | 0 | 2 | 3 | false |
| P60983 | 0.66 | GMFB | Glia maturation factor beta | false | 1 | 2 | 1 | false |
| ***Protein up-regulated by LPS*** | | | | | | | | |
| Q96AT9 | 51.49 | RPE | Ribulose-phosphate 3-epimerase | false | 0 | 0 | 3 | false |
| O14684 | 4.09 | PTGES | Prostaglandin E synthase | false | 8 | 4 | 0 | false |

**Table 1** (continued)

| Accession | Group Profile (Ratio) | Gene names (primary) | Description | OA associated | human OA DEG | induced OA DEG | OA gene interaction | skeletal phenotype |
|---|---|---|---|---|---|---|---|---|
| P43490 | 3.35 | NAMPT | Nicotinamide phphoribyltransferase | true | 8 | 0 | 4 | false |
| O43776 | 2.66 | NARS1 | Asparagine--tRNA ligase cytoplasmic | false | 0 | 0 | 3 | false |
| Q5VYK3 | 2.56 | ECPAS | Proteasome adapter and scaffold protein ECM29 | false | 1 | 0 | 8 | false |
| P12955 | 2.47 | PEPD | Xaa-Pro dipeptidase | false | 0 | 5 | 5 | true |
| P10301 | 2.33 | RRAS | Ras-related protein R-Ras | false | 3 | 1 | 5 | false |
| P19827 | 2.27 | ITIH1 | Inter-alpha-trypsin inhibitor heavy chain H1 | false | 0 | 1 | 1 | false |
| P15121 | 2.04 | AKR1B1 | Aldo-keto reductase family 1 member B1 | false | 0 | 4 | 3 | false |
| O14828 | 1.96 | SCAMP3 | Secretory carrier-associated membrane protein 3 | false | 1 | 1 | 4 | false |
| P07711 | 1.95 | CTSL | Cathepsin L1 | false | 4 | 0 | 3 | false |
| Q6IBS0 | 1.92 | TWF2 | Twinfilin-2 | false | 0 | 5 | 0 | false |
| P04179 | 1.9 | SOD2 | Superoxide dismutase [Mn] mitochondrial | true | 7 | 7 | 8 | false |
| P54709 | 1.85 | ATP1B3 | Sodium/potassium-transporting ATPase subunit beta-3 | false | 1 | 3 | 3 | false |
| Q9Y3Z3 | 1.84 | SAMHD1 | Deoxynucleide triphphate triphphohydrolase SAMHD1 | false | 1 | 2 | 3 | false |
| Q9Y3A6 | 1.84 | TMED5 | Transmembrane emp24 domain-containing protein 5 | false | 3 | 3 | 0 | false |
| Q13501 | 1.79 | SQSTM1 | Sequestome-1 | false | 3 | 1 | 42 | true |
| Q96JJ7 | 1.79 | TMX3 | Protein disulfide-isomerase TMX3 | false | 0 | 0 | 0 | false |
| O75828 | 1.78 | CBR3 | Carbonyl reductase [NADPH] 3 | false | 2 | 5 | 3 | false |
| P35613 | 1.78 | BSG | Basigin | false | 2 | 0 | 7 | false |
| P26599 | 1.76 | PTBP1 | Polypyrimidine tract-binding protein 1 | false | 2 | 0 | 11 | false |
| Q9Y295 | 1.76 | DRG1 | Developmentally-regulated GTP-binding protein 1 | false | 0 | 1 | 2 | false |
| Q7L523 | 1.74 | RRAGA | Ras-related GTP-binding protein A | false | 0 | 3 | 2 | false |
| P61009 | 1.7 | SPCS3 | Signal peptidase complex subunit 3 | false | 2 | 1 | 1 | false |
| Q96HE7 | 1.69 | ERO1A | ERO1-like protein alpha | false | 5 | 1 | 1 | false |
| Q9UL46 | 1.66 | PSME2 | Proteasome activator complex subunit 2 | false | 0 | 0 | 2 | false |
| Q13724 | 1.63 | MOGS | Mannyl-oligaccharide glucidase | false | 0 | 2 | 5 | false |
| Q9Y5P6 | 1.63 | GMPPB | Manne-1-phphate guanyltransferase beta | false | 2 | 2 | 1 | false |
| P19525 | 1.61 | EIF2AK2 | Interferon-induced double-stranded RNA-activated protein kinase | false | 1 | 1 | 18 | false |
| P02794 | 1.59 | FTH1 | Ferritin heavy chain | false | 3 | 1 | 5 | false |
| P18085 | 1.58 | ARF4 | ADP-ribylation factor 4 | false | 2 | 10 | 10 | false |
| P23381 | 1.57 | WARS1 | Tryptophan--tRNA ligase cytoplasmic | false | 0 | 0 | 3 | false |
| P63244 | 1.56 | RACK1 | Receptor of activated protein C kinase 1 | false | 1 | 0 | 22 | false |
| Q9NZ08 | 1.56 | ERAP1 | Endoplasmic reticulum aminopeptidase 1 | false | 1 | 1 | 3 | false |

**Table 1** (continued)

| Accession | Group Profile (Ratio) | Gene names (primary) | Description | OA associated | human OA DEG | induced OA DEG | OA gene interaction | skeletal phenotype |
|---|---|---|---|---|---|---|---|---|
| O95747 | 1.55 | OXSR1 | Serine/threonine-protein kinase R1 | false | 1 | 1 | 6 | false |
| P17858 | 1.54 | PFKL | ATP-dependent 6-phphofruc-tokinase liver type | false | 1 | 3 | 6 | false |
| P08195 | 1.53 | SLC3A2 | 4F2 cell-surface antigen heavy chain | false | 6 | 0 | 7 | false |
| Q9UNN8 | 1.53 | PROCR | Endothelial protein C receptor | false | 4 | 8 | 0 | false |
| P04439 | 1.51 | HLA-A | HLA class I histocompatibility antigen A alpha chain | false | 1 | 0 | 5 | false |
| P50991 | 1.5 | CCT4 | T-complex protein 1 subunit delta | false | 0 | 3 | 11 | false |

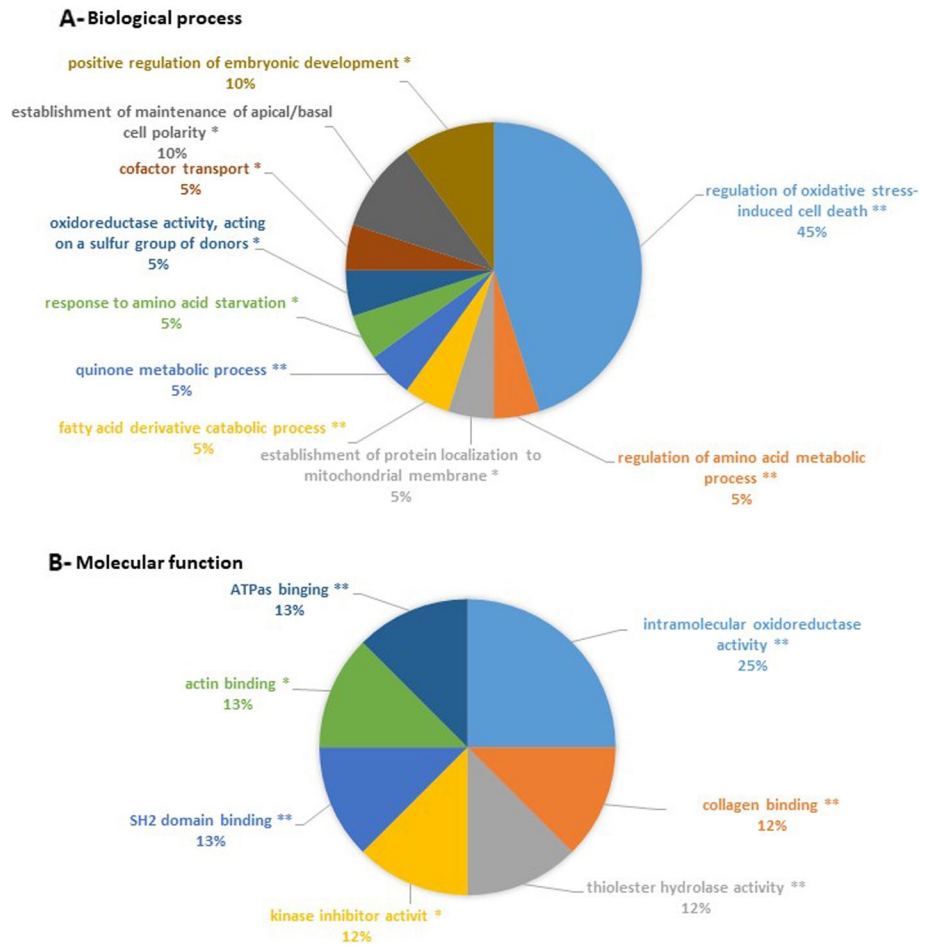


**Fig. 2** Enrichment in the biological process and molecular function. From differentially expressed proteins between the control group and the LPS group (Fig. 1), enrichments in a biological process (**A**) and molecular process (**B**) were performed. The diagram shows part of each GO Term, which were statistically enriched. *: $p$-value< 0.05, **: $p$-value< 0.01

**Table 2** Enrichment in biological processes

| GOID | GOTerm | Term PValue | % Associated Genes | Nr. Genes | Associated Genes Found |
|---|---|---|---|---|---|
| GO:0006521 | regulation of cellular amino acid metabolic process | 0.007 | 4.48 | 3 | [BSG, PSMD6, PSME2] |
| GO:0016667 | oxidoreductase activity, acting on a sulfur group of donors | 0.005 | 5.00 | 3 | [ERO1A, TMX3, TXNDC17] |
| GO:0071230 | cellular response to amino acid stimulus | 0.001 | 5.56 | 4 | [ASS1, COL6A1, LAMTOR5, RRAGA] |
| GO:0072523 | purine-containing compound catabolic process | 0.004 | 5.36 | 3 | [ACOT7, PNP, SAMHD1] |
| GO:1901569 | fatty acid derivative catabolic process | 0.000 | 18.75 | 3 | [ACOT7, LYPLA2, OXCT1] |
| GO:1901661 | quinone metabolic process | 0.001 | 8.11 | 3 | [AKR1B1, CBR3, NDUFA9] |
| GO:1990928 | response to amino acid starvation | 0.003 | 5.88 | 3 | [EIF2AK2, FASN, RRAGA] |
| GO:0034198 | cellular response to amino acid starvation | 0.003 | 6.25 | 3 | [EIF2AK2, FASN, RRAGA] |
| GO:0070671 | response to interleukin-12 | 0.005 | 5.08 | 3 | [CDC42, PSME2, SOD2] |
| GO:0035722 | interleukin-12-mediated signaling pathway | 0.004 | 5.36 | 3 | [CDC42, PSME2, SOD2] |
| GO:0040019 | positive regulation of embryonic development | 0.002 | 6.98 | 3 | [AKR1B1, OXSR1, RACK1] |
| GO:0071470 | cellular response to osmotic stress | 0.004 | 5.66 | 3 | [AKR1B1, LETM1, OXSR1] |
| GO:0051181 | cofactor transport | 0.005 | 5.17 | 3 | [BSG, OXSR1, SLC9A3R1] |
| GO:0072337 | modified amino acid transport | 0.001 | 10.00 | 3 | [BSG, OXSR1, SLC9A3R1] |
| GO:0061245 | establishment or maintenance of bipolar cell polarity | 0.004 | 5.66 | 3 | [ARF4, CDC42, SLC9A3R1] |
| GO:0035088 | establishment or maintenance of apical/basal cell polarity | 0.004 | 5.66 | 3 | [ARF4, CDC42, SLC9A3R1] |
| GO:0045197 | establishment or maintenance of epithelial cell apical/basal polarity | 0.003 | 6.25 | 3 | [ARF4, CDC42, SLC9A3R1] |
| GO:0007006 | mitochondrial membrane organization | 0.000 | 4.05 | 6 | [ATP5PB, HSPA4, LETM1, MTX2, NMT1, TIMM13] |
| GO:0051205 | protein insertion into membrane | 0.007 | 4.48 | 3 | [HSPA4, NMT1, TIMM13] |
| GO:0090151 | establishment of protein localization to mitochondrial membrane | 0.003 | 5.88 | 3 | [HSPA4, NMT1, TIMM13] |
| GO:0051204 | protein insertion into mitochondrial membrane | 0.003 | 6.38 | 3 | [HSPA4, NMT1, TIMM13] |
| GO:1902882 | regulation of response to oxidative stress | 0.000 | 4.90 | 5 | [BSG, NONO, RACK1, SOD2, UBQLN1] |
| GO:1902883 | negative regulation of response to oxidative stress | 0.000 | 6.67 | 4 | [BSG, NONO, RACK1, SOD2] |
| GO:0036473 | cell death in response to oxidative stress | 0.000 | 5.00 | 5 | [BSG, NONO, RACK1, SOD2, UBQLN1] |
| GO:1900407 | regulation of cellular response to oxidative stress | 0.000 | 5.38 | 5 | [BSG, NONO, RACK1, SOD2, UBQLN1] |
| GO:1900408 | negative regulation of cellular response to oxidative stress | 0.000 | 6.90 | 4 | [BSG, NONO, RACK1, SOD2] |
| GO:0008631 | intrinsic apoptotic signaling pathway in response to oxidative stress | 0.003 | 6.25 | 3 | [NONO, SOD2, UBQLN1] |
| GO:1903201 | regulation of oxidative stress-induced cell death | 0.000 | 6.33 | 5 | [BSG, NONO, RACK1, SOD2, UBQLN1] |
| GO:0036475 | neuron death in response to oxidative stress | 0.001 | 9.09 | 3 | [BSG, NONO, RACK1] |
| GO:1903202 | negative regulation of oxidative stress-induced cell death | 0.000 | 6.90 | 4 | [BSG, NONO, RACK1, SOD2] |
| GO:1903203 | regulation of oxidative stress-induced neuron death | 0.001 | 10.00 | 3 | [BSG, NONO, RACK1] |
| GO:1902175 | regulation of oxidative stress-induced intrinsic apoptotic signaling pathway | 0.001 | 9.68 | 3 | [NONO, SOD2, UBQLN1] |
| GO:1903204 | negative regulation of oxidative stress-induced neuron death | 0.000 | 13.64 | 3 | [BSG, NONO, RACK1] |

**Table 3** Enrichment in molecular functions

| GOID | GOTerm | Term PValue | % Associated Genes | Nr. Genes | Associated Genes Found |
|---|---|---|---|---|---|
| GO:0005518 | collagen binding | 0.009 | 4.05 | 3 | [COL6A1, CTSL, THBS1] |
| GO:0016790 | thiolester hydrolase activity | 0.000 | 10.00 | 4 | [ACOT7, ACOT9, FASN, LYPLA2] |
| GO:0019210 | kinase inhibitor activity | 0.008 | 4.29 | 3 | [GMFB, RACK1, WARS1] |
| GO:0042169 | SH2 domain binding | 0.002 | 6.52 | 3 | [KHDRBS1, RACK1, SQSTM1] |
| GO:0042805 | actinin binding | 0.002 | 6.98 | 3 | [LMO7, PALLD, PDLIM7] |
| GO:0051117 | ATPase binding | 0.002 | 4.30 | 4 | [AKR1B1, ATP1B3, ATP6V1G1, NSFL1C] |
| GO:0016667 | oxidoreductase activity, acting on a sulfur group of donors | 0.005 | 5.00 | 3 | [ERO1A, TMX3, TXNDC17] |
| GO:0016860 | intramolecular oxidoreductase activity | 0.000 | 6.67 | 4 | [ERO1A, GNPDA2, PTGES, TMX3] |

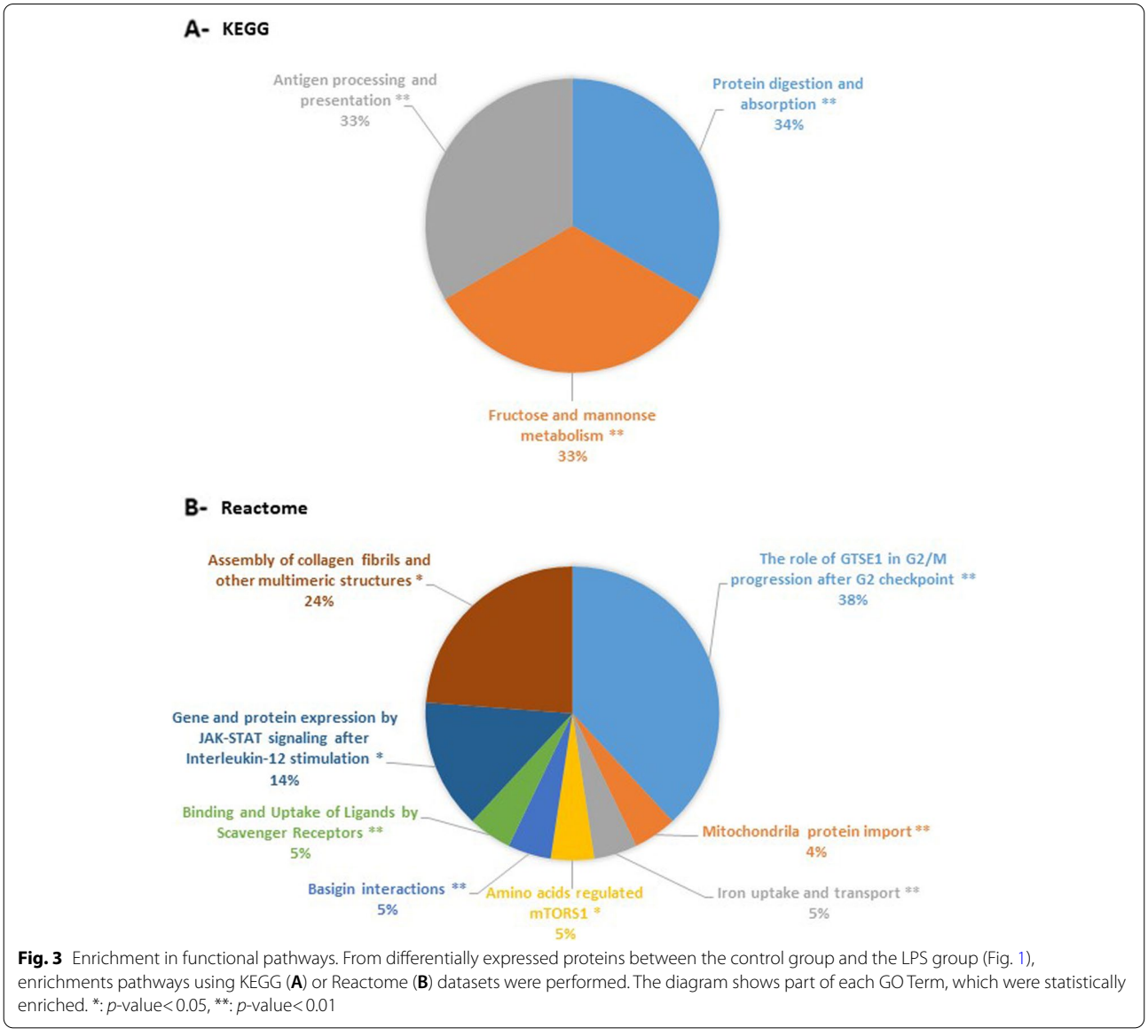


**Fig. 3** Enrichment in functional pathways. From differentially expressed proteins between the control group and the LPS group (Fig. 1), enrichments pathways using KEGG (**A**) or Reactome (**B**) datasets were performed. The diagram shows part of each GO Term, which were statistically enriched. *: *p*-value< 0.05, **: *p*-value< 0.01

**Table 4** Enrichment using KEGG

| GOID | GOTerm | Term PValue | % Associated Genes | Nr. Genes | Associated Genes Found |
|---|---|---|---|---|---|
| KEGG:00051 | Fructose and mannose metabolism | 0.002 | 9.09 | 3 | [AKR1B1, GMPPB, PFKL] |
| KEGG:04612 | Antigen processing and presentation | 0.003 | 5.13 | 4 | [CTSL, HLA-A, HSPA4, PSME2] |
| KEGG:04974 | Protein digestion and absorption | 0.005 | 4.21 | 4 | [ATP1B3, COL6A1, COL6A3, SLC3A2] |

**Table 5** Enrichment using reactome

| GOID | GOTerm | Term PValue | % Associated Genes | Nr. Genes | Associated Genes Found |
|---|---|---|---|---|---|
| R-HSA:1268020 | Mitochondrial protein import | 0.001 | 6.25 | 4 | [MTX2, PITRM1, TIMM13, TOMM70] |
| R-HSA:917937 | Iron uptake and transport | 0.009 | 5.17 | 3 | [ATP6V1G1, FTH1, NEDD8] |
| R-HSA:9639288 | Amino acids regulate mTORC1 | 0.008 | 5.45 | 3 | [ATP6V1G1, LAMTOR5, RRAGA] |
| R-HSA:210991 | Basigin interactions | 0.001 | 12.00 | 3 | [ATP1B3, BSG, SLC3A2] |
| R-HSA:2173782 | Binding and Uptake of Ligands by Scavenger Receptors | 0.000 | 9.52 | 4 | [ALB, FTH1, HBA1, HSPH1] |
| R-HSA:447115 | Interleukin-12 family signaling | 0.009 | 5.26 | 3 | [CDC42, PSME2, SOD2] |
| R-HSA:8950505 | Gene and protein expression by JAK-STAT signaling after Interleukin-12 stimulation | 0.003 | 7.89 | 3 | [CDC42, PSME2, SOD2] |
| R-HSA:9020591 | Interleukin-12 signaling | 0.005 | 6.38 | 3 | [CDC42, PSME2, SOD2] |
| R-HSA:1442490 | Collagen degradation | 0.012 | 4.69 | 3 | [COL6A1, COL6A3, CTSL] |
| R-HSA:1474290 | Collagen formation | 0.005 | 4.44 | 4 | [CD151, COL6A1, COL6A3, CTSL] |
| R-HSA:186797 | Signaling by PDGF | 0.009 | 5.17 | 3 | [COL6A1, COL6A3, THBS1] |
| R-HSA:2022090 | Assembly of collagen fibrils and other multimeric structures | 0.001 | 6.56 | 4 | [CD151, COL6A1, COL6A3, CTSL] |
| R-HSA:216083 | Integrin cell surface interactions | 0.004 | 4.71 | 4 | [BSG, COL6A1, COL6A3, THBS1] |
| R-HSA:1632852 | Macroautophagy | 0.001 | 4.41 | 6 | [LAMTOR5, RRAGA, SQSTM1, TOMM70, TUBA1A, TUBB1] |
| R-HSA:2995410 | Nuclear Envelope (NE) Reassembly | 0.019 | 4.00 | 3 | [BANF1, TUBA1A, TUBB1] |
| R-HSA:389957 | Prefoldin mediated transfer of substrate to CCT/TriC | 0.001 | 10.71 | 3 | [CCT4, TUBA1A, TUBB1] |
| R-HSA:389958 | Cooperation of Prefoldin and TriC/CCT in actin and tubulin folding | 0.002 | 9.38 | 3 | [CCT4, TUBA1A, TUBB1] |
| R-HSA:389960 | Formation of tubulin folding intermediates by CCT/TriC | 0.001 | 12.00 | 3 | [CCT4, TUBA1A, TUBB1] |
| R-HSA:5626467 | RHO GTPases activate IQGAPs | 0.002 | 9.38 | 3 | [CDC42, TUBA1A, TUBB1] |
| R-HSA:8852276 | The role of GTSE1 in G2/M progression after G2 checkpoint | 0.000 | 6.49 | 5 | [MAPRE1, PSMD6, PSME2, TUBA1A, TUBB1] |
| R-HSA:9663891 | Selective autophagy | 0.003 | 4.94 | 4 | [SQSTM1, TOMM70, TUBA1A, TUBB1] |

Jaccard (sig) = 0.0118; z score = 3.98). In addition, using OATargets databases [34], we were able to observe that several identified proteins were encoded by genes associated with OA, such as Thrombpondin-1 (THBS1), collagen alpha-1(VI) chain (COL6A1), superoxide dismutase [Mn] mitochondrial (SOD2) and Nicotinamide phosphoribosyltransferase (NAMPT) (Table 1). In addition, about half of these genes were also found at least once as a human OA DEG, and around 90% are known to interact with OA genes (Table 1).

Altogether, this proteomic analysis clearly confirms that LPS-stimulated synovial cells from OA human patients are a good model for studying the osteoarthritis process in vitro.

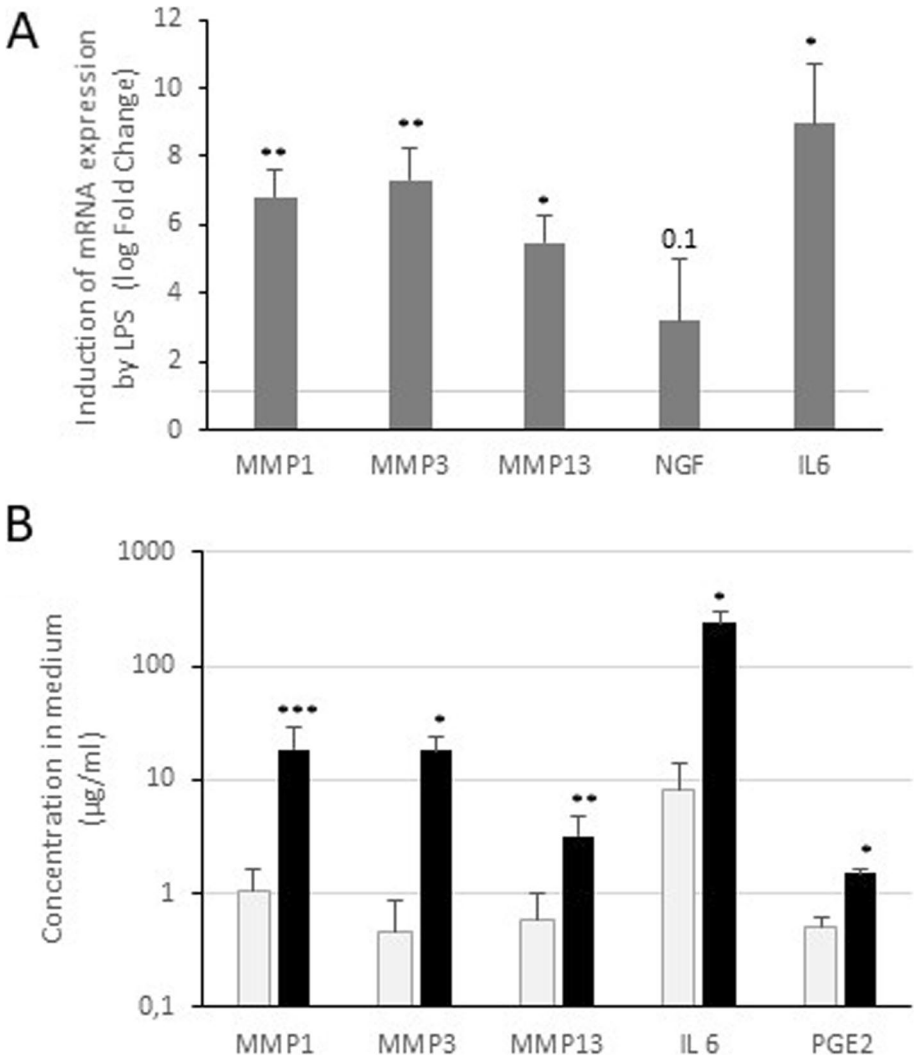


**Fig. 4** LPS induces gene expression and release in medium of catabolism, inflammation and pain markers. Human synovial cells were treated with LPS (1 µg/ml) for 24 h. **A** - At the end of the experiments, RNA was extracted. Relative mRNA expression of MMP-1, MMP-3, MMP-13, NGF and IL-6 was determined by RT-PCR. Values are compared to untreated cells and presented as a log Fold Change (compared to the control group). **B** - Culture media were collected and ELISA was performed to assayed MMP, IL-6 and PGE2 concentration in medium. Values are expressed as µg/ml medium ($n = 4$). *: $p$-value< 0.05, **: $p$-value< 0.01, ***: $p$-value< 0.001

### LPS increases the expression of genes associated with inflammation, catabolism and pain

Next, using a commonly targeted strategy, we investigated the effect of LPS treatment in human OA synovial cells. After 24 h of treatment, LPS stimulated inflammation through the production of pro-inflammatory cytokines (Interleukin-6, IL-6), catabolism through an increase of metalloproteases (MMP-1, MMP-3, MMP-13), and the production of pain-mediating neurotrophin (Nerve Growth Factor, NGF). These increases were observed in terms of mRNA levels and protein release. LPS also increased the amount of PGE2, another pain mediator (Fig. 4).

### The combination of curcumin with bromelain and harpagophytum significantly reduced the LPS-induced expression of genes associated with catabolism

Having validated our model, we continued by studying the effect of vegetal extracts (curcumin bromelain and harpagophytum) on OA-associated genes. On the doses tested, vegetal extracts had little effect on the expression of catabolic genes. Only curcumin slightly counteracted the effects of LPS on MMP-13 mRNA and protein release. However, the combination of curcumin with bromelain and harpagophytum reversed the effects of LPS on the mRNA levels of MMP-1, MMP-3 and MMP-13, and on the release

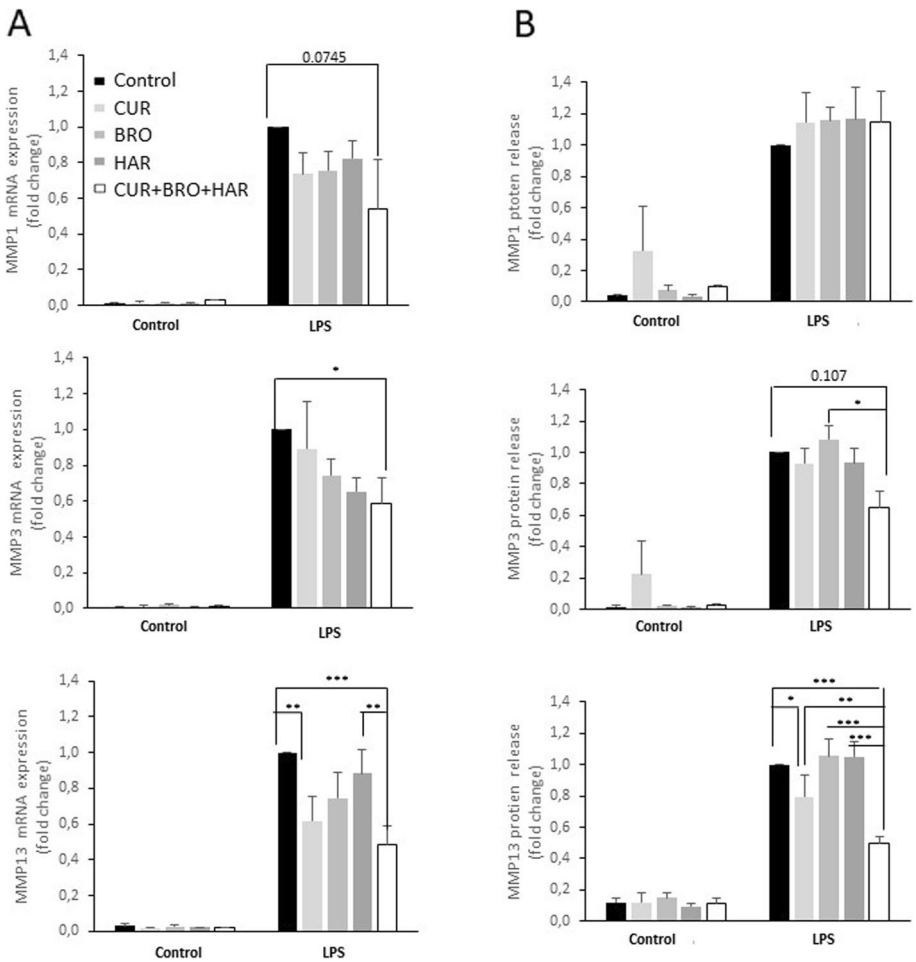


**Fig. 5** The combination of curcumin with bromelain and harpagophytum significantly reduced the LPS-induced expression of genes associated with catabolism. Human synovial cells were treated with LPS (1 µg/ml) for 24 h in the presence of curcumin (CUR, 13 µM), bromelain (BRO, 14.7 µg/ml) and harpagophytum (HAR, 36 µg/ml), and all three together. **A** - At the end of the experiments, RNA was extracted and media collected. Relative mRNA expression of MMP-1, MMP-3 and MMP-13 was determined by RT-PCR. **B** - Culture media were also collected and ELISA performed to assayed MMP release in medium. Values were compared to LPS-treated cells and presented as relative expression (compared to the LPS group). $n = 3$. *: $p$-value< 0.05, **: $p$-value< 0.01, ***: $p$-value< 0.001

of MMP-3 and MMP-13 proteins (Fig. 5). These data suggested that the combination of curcumin, bromelain and harpagophytum may reduce cartilage degradation during the OA process.

### The combination of curcumin with bromelain and harpagophytum significantly reduced the LPS-induced expression of genes associated with inflammation and pain

Next, we investigated the effect of these vegetal compounds on the expression of genes involved in inflammation and pain (Fig. 6). We observed that only curcumin was able to slightly reduce the LPS-induced expression of NGF and the release of PGE2 and IL-6. Interestingly, the combination of all three vegetal compounds (curcumin, bromelain and harpagophytum) significantly reduced the gene expression of IL-6 and NGF mRNA expression. It also decreased the IL-6 release and the production of PGE2. This suggests that the combination of these three compounds may reduce inflammation and pain.

## Discussion

To date, no efficient treatment exists to reverse osteoarthritis. As a result, it is crucial that we identify strategies that can slow down OA progression and that are usable in the long term. Some natural compounds are known to present anti-oxidative and anti-inflammatory actions, so they may be an alternative to pharmacological drugs. In this study, after proteomic characterisation of the in vitro OA model which was used, and after confirming that it

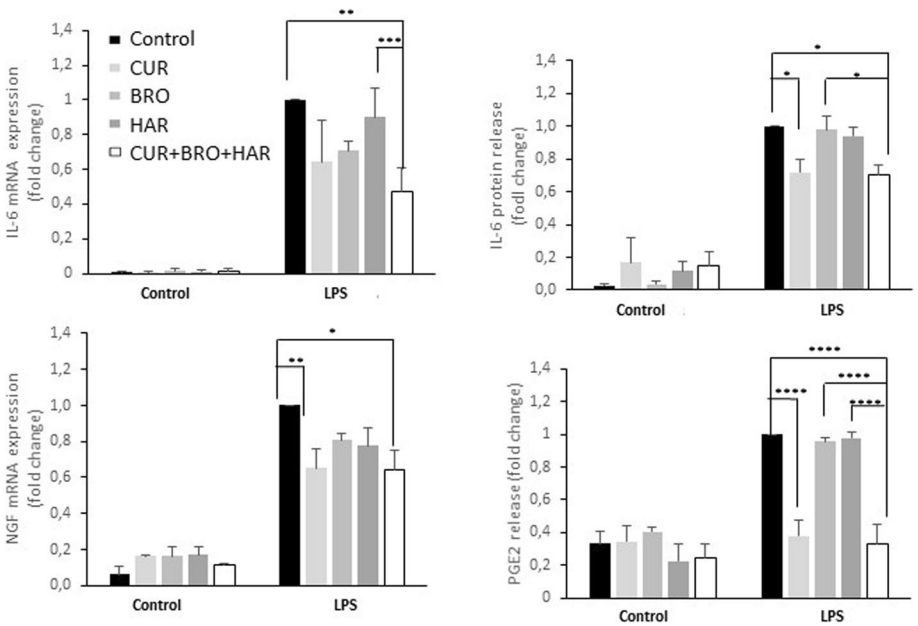


**Fig. 6** The combination of curcumin with bromelain and harpagophytum significantly reduced the LPS-induced expression of genes associated with inflammation and pain. Human synovial cells were treated with LPS (1 µg/ml) for 24 h in the presence of curcumin (CUR, 13 µM), bromelain (BRO, 14.7 µg/ml) and harpagophytum (HAR, 36 µg/ml), and all three together. At the end of the experiments, RNA were extracted and the media collected. Relative mRNA expression of NGF and IL-6 were determined by RT-PCR. Culture media were also collected and ELISA performed to assayed IL-6 and PGE2 release in medium. Values were compared to LPS-treated cells and presented as relative release (compared to the LPS group). $n = 3$. *: $p$-value< 0.05, **: $p$-value< 0.01, ***: $p$-value< 0.001

was able to induce changes in gene expression profiles similar to that observed during OA, we demonstrated that the combination of curcumin, and bromelain and harpagophytum is efficient in counteracting numerous LPS-induced effects in human OA synovial cells.

Firstly, we evaluated the potential of lipopolysaccharide to induce changes in gene/protein expression by mimicking some features of OA. LPS is an endotoxin and a classical activator of the innate immune system. Because of its pathophysiological properties, LPS has been used to induce arthritis in conjunction with collagen in animal models [37, 38]. More recently, researchers have started to connect LPS with the pathogenesis of OA [39]. LPS is released by gut microbiota and is correlated with the pathophysiology of osteoarthritis, in part through the activation of macrophages. In addition, local LPS administration to joints induces synovitis and is used as a model to evaluate potential treatments for acute synovitis [40].

Since LPS is now considered a trigger for OA pathology, especially by activating synovial cells, we have proposed that stimulated human OA synovial cells may induce inflammation and reproduce in vitro some changes observed during the OA process. Using proteomics, we demonstrated here that treating human OA synovial cells with LPS induces the expression of OA signature genes, and in particular reproduces some gene expression changes observed in synovial cells from inflammatory and normal areas of the osteoarthritis synovial membrane. A more targeted strategy showed, for instance, that LPS induced the expression of MMPs, IL-6, PGE2 and NGF, which are mainly markers of catabolism, inflammation and joint pain. Consequently, the stimulation of human OA synovial cells by LPS appeared to be a good in vitro model for studying inflammation during OA. With the knowledge that alleviating inflammation may prevent the onset or minimise the progression of OA [2, 14, 15, 39], we suggested the use of this in vitro model to test the ability of several natural substances to reduce inflammation.

Firstly, we demonstrated that curcumin has some anti-catabolic and anti-inflammatory effects in human OA synovial cells. This correlates with the literature, which demonstrates that curcumin reduces MMP-3 and MMP-13 expression in rabbit chondrocytes and in the articular cartilage of oestrogen-deficient rats, preventing collagen degradation [41, 42]. Also, curcumin prevents the activation of nuclear factor kappa B (NF-κB), the major mediator of inflammation [42, 43]. Another study shows that curcumin favours cartilage anabolism by increasing type II collagen synthesis [25, 44].

We also investigated the effects of *harpagophytum*, commonly known as devil's claw, a plant used worldwide as a traditional remedy for joint pain associated with OA and mild rheumatic ailments [28, 45, 46]. Moreover, it has been described as having analgesic effects on neuropathic pain in rats [47]. We also studied the effects of bromelain, a food supplement that is sometimes described as an alternative treatment to nonsteroidal anti-inflammatory drugs (NSAIDs) [48]. Bromelain has analgesic properties [49, 50] and relieves OA symptoms [27]. However, at the dose tested, neither harpagophytum nor bromelain showed significant effects on the expression of studied genes, including NGF or PGE2, which are known to be related to joint pain. However, the combination of these vegetal components with curcumin may counteract numerous LPS effects in human OA-stimulated cells. The combination of curcumin with bromelain and harpagophytum significantly reduced the LPS-induced expression of genes associated with inflammation and pain, but also catabolism. This reinforced action of curcumin in combination with other natural compounds has already been seen [18]. For instance, the combination treatment of *Lactobacillus acidophilus* LA-1, vitamin B and curcumin ameliorates the progression of osteoarthritis by inhibiting the pro-inflammatory mediators [26]. However, to our knowledge, this paper is the first to show the benefits of combining curcumin with bromelain and harpagophytum.

In conclusion, we have described the changes in protein expression induced by LPS in human OA synovial cells and demonstrated that they are characteristic of inflamed OA synoviocytes, suggesting that this in vitro model may be useful for evaluating inflammation during OA. In addition, we have shown that the combination of three natural vegetal components reduced the expression of genes involved in catabolism, inflammation and pain, suggesting that together, they may present a beneficial effect on OA patients by alleviating OA pain and synovial inflammation and reducing cartilage degradation.

## Supplementary Information

The online version contains supplementary material available at https://doi.org/10.1186/s12906-021-03435-7.

**Additional file 1.**

**Acknowledgments**
The authors would like to thank Sylvain Leclercq and collaborators (Clinique Saint-Martin, Caen, France) for the gift of the synovial tissues.

**Authors' contributions**
CB participated in the conception, design of the study, data analysis and drafted the manuscript. SB carried out the experiments and data analysis. BB and JP conducted the proteomic experiments and analysis. TC participated in the coordination and conception of the study and design. KB participated in the conception and design of the study and helped to draft the manuscript. All authors read and approved the final manuscript.

**Funding**
This study was funded by Labrha laboratory, which also supplied the vegetal compounds. The funding laboratory had no role in the study design, data collection and analysis, decision to publish, or preparation of the manuscript.

**Availability of data and materials**
The datasets supporting the conclusions of this article are included within the article and its additional file.

## Declarations

**Ethics approval and consent to participate**
The experimental protocol was approved by the local ethical committee 'Comité de Protection des Personnes Nord-Ouest III' (authorisation # A13-D46-VOL.19). The informed consent of each participant was obtained prior to surgery. They all signed consent forms, in accordance with local law. All methods were performed in accordance with the relevant guidelines and regulations.

**Consent for publication**
Not applicable.

**Competing interests**
Thierry Conrozier received fees from LABRHA for scientific consulting and speaking services.
The other authors declare that they have no competing interests.

**Author details**
[1]EA7451 BioConnect, Université de Caen Normandie, UNICAEN, 14032 Caen, France. [2]Proteogen platform, Normandie Univ, UNICAEN, Caen, France. [3]Rheumatology Department, Nord Franche-Comté Hospital, Trevenans, France.

Received: 31 March 2021 Accepted: 27 September 2021
Published online: 14 October 2021

**References**

1. Malemud CJ. Biologic basis of osteoarthritis: state of the evidence. Curr Opin Rheumatol. 2015;27:289–94.
2. Berenbaum F. Osteoarthritis as an inflammatory disease (osteoarthritis is not osteoarthrosis!). Osteoarthr Cartil. 2013;21:16–21.
3. Neogi T. The epidemiology and impact of pain in osteoarthritis. Osteoarthr Cartil. 2013;21:1145–53.
4. Robinson WH, Lepus CM, Wang Q, Raghu H, Mao R, Lindstrom TM, et al. Low-grade inflammation as a key mediator of the pathogenesis of osteoarthritis. Nat Rev Rheumatol. 2016;12:580–92.
5. Bigoni M, Sacerdote P, Turati M, Franchi S, Gandolla M, Gaddi D, et al. Acute and late changes in intraarticular cytokine levels following anterior cruciate ligament injury. J Orthop Res Off Publ Orthop Res Soc. 2013;31:315–21.
6. Kapoor M, Martel-Pelletier J, Lajeunesse D, Pelletier J-P, Fahmi H. Role of proinflammatory cytokines in the pathophysiology of osteoarthritis. Nat Rev Rheumatol. 2011;7:33–42.
7. Scotece M, Conde J, Abella V, López V, Francisco V, Ruiz C, et al. Oleocanthal inhibits catabolic and inflammatory mediators in LPS-activated human primary osteoarthritis (OA) chondrocytes through MAPKs/NF-κB pathways. Cell Physiol Biochem Int J Exp Cell Physiol Biochem Pharmacol. 2018;49:2414–26.
8. Konttinen YT, Sillat T, Barreto G, Ainola M, Nordström DCE. Osteoarthritis as an autoinflammatory disease caused by chondrocyte-mediated inflammatory responses. Arthritis Rheum. 2012;64:613–6.
9. Di Paola R, Fusco R, Impellizzeri D, Cordaro M, Britti D, Morittu VM, et al. Adelmidrol, in combination with hyaluronic acid, displays increased anti-inflammatory and analgesic effects against monosodium iodoacetate-induced osteoarthritis in rats. Arthritis Res Ther. 2016;18:291.

10. Cordaro M, Siracusa R, Impellizzeri D, D' Amico R, Peritore AF, Crupi R, et al. Safety and efficacy of a new micronized formulation of the ALIAmide palmitoylglucosamine in preclinical models of inflammation and osteoarthritis pain. Arthritis Res Ther. 2019;21:254.
11. Fusco R, Siracusa R, Peritore AF, Gugliandolo E, Genovese T, D'Amico R, et al. The Role of Cashew (*Anacardium occidentale* L.) Nuts on an Experimental Model of Painful Degenerative Joint Disease. Antioxidants. 2020;9:511.
12. Xiao Y, Ding L, Yin S, Huang Z, Zhang L, Mei W, et al. Relationship between the pyroptosis of fibroblast-like synoviocytes and HMGB1 secretion in knee osteoarthritis. Mol Med Rep. 2021;23:1.
13. Santangelo KS, Nuovo GJ, Bertone AL. In vivo reduction or blockade of interleukin-1β in primary osteoarthritis influences expression of mediators implicated in pathogenesis. Osteoarthr Cartil. 2012;20:1610–8.
14. Griffin TM, Huebner JL, Kraus VB, Yan Z, Guilak F. Induction of osteoarthritis and metabolic inflammation by a very high-fat diet in mice: effects of short-term exercise. Arthritis Rheum. 2012;64:443–53.
15. Huang Z, Kraus VB. Does lipopolysaccharide-mediated inflammation have a role in OA? Nat Rev Rheumatol. 2016;12:123–9.
16. Li K, Liu A, Zong W, Dai L, Liu Y, Luo R, et al. Moderate exercise ameliorates osteoarthritis by reducing lipopolysaccharides from gut microbiota in mice. Saudi J Biol Sci. 2021;28:40–9.
17. Tabas I, Glass CK. Anti-inflammatory therapy in chronic disease: challenges and opportunities. Science. 2013;339:166–72.
18. Hosseini-Zare MS, Sarhadi M, Zarei M, Thilagavathi R, Selvam C. Synergistic effects of curcumin and its analogs with other bioactive compounds: a comprehensive review. Eur J Med Chem. 2021;210:113072.
19. Henrotin Y, Malaise M, Wittoek R, de Vlam K, Brasseur J-P, Luyten FP, et al. Bio-optimized Curcuma longa extract is efficient on knee osteoarthritis pain: a double-blind multicenter randomized placebo controlled three-arm study. Arthritis Res Ther. 2019;21. https://doi.org/10.1186/s13075-019-1960-5.
20. Madhu K, Chanda K, Saji MJ. Safety and efficacy of Curcuma longa extract in the treatment of painful knee osteoarthritis: a randomized placebo-controlled trial. Inflammopharmacology. 2013;21:129–36.
21. Atabaki M, Shariati-Sarabi Z, Tavakkol-Afshari J, Mohammadi M. Significant immunomodulatory properties of curcumin in patients with osteoarthritis; a successful clinical trial in Iran. Int Immunopharmacol. 2020;85:106607.
22. Nakagawa Y, Mukai S, Yamada S, Murata S, Yabumoto H, Maeda T, et al. The efficacy and safety of highly-bioavailable Curcumin for treating knee osteoarthritis: a 6-month open-labeled prospective study. Clin Med Insights Arthritis Musculoskelet Disord. 2020;13:1179544120948471.
23. Belcaro G, Cesarone MR, Dugall M, Pellegrini L, Ledda A, Grossi MG, et al. Efficacy and safety of Meriva®, a curcumin-phosphatidylcholine complex, during extended administration in osteoarthritis patients. Altern Med Rev J Clin Ther. 2010;15:337–44.
24. Yeh C-C, Su Y-H, Lin Y-J, Chen P-J, Shi C-S, Chen C-N, et al. Evaluation of the protective effects of curcuminoid (curcumin and bisdemethoxycurcumin)-loaded liposomes against bone turnover in a cell-based model of osteoarthritis. Drug Des Devel Ther. 2015;9:2285–300.
25. Nicoliche T, Maldonado DC, Faber J, da Silva MCP. Evaluation of the articular cartilage in the knees of rats with induced arthritis treated with curcumin. PLoS One. 2020;15:e0230228.
26. Jhun J, Min H-K, Na HS, Kwon JY, Ryu J, Cho K-H, et al. Combinatmarion treatment with lactobacillus acidophilus LA-1, vitamin B, and curcumin ameliorates the progression of osteoarthritis by inhibiting the pro-inflammatory mediators. Immunol Lett. 2020;228:112–21.
27. Pavan R, Jain S, Null S, Kumar A. Properties and therapeutic application of bromelain: a review. Biotechnol Res Int. 2012;2012:976203.
28. Mariano A, Di Sotto A, Leopizzi M, Garzoli S, Di Maio V, Gullì M, et al. Antiarthritic effects of a root extract from Harpagophytum procumbens DC: novel insights into the molecular mechanisms and possible bioactive phytochemicals. Nutrients. 2020;12:2545.
29. Allas L, Brochard S, Rochoux Q, Ribet J, Dujarrier C, Veyssiere A, et al. EZH2 inhibition reduces cartilage loss and functional impairment related to osteoarthritis. Sci Rep. 2020;10:19577.
30. Fischer R, Kessler BM. Gel-aided sample preparation (GASP)—a simplified method for gel-assisted proteomic sample generation from protein extracts and intact cells. Proteomics. 2015;15:1224–9.
31. Meier F, Brunner A-D, Koch S, Koch H, Lubeck M, Krause M, et al. Online parallel accumulation-serial fragmentation (PASEF) with a novel trapped ion mobility mass spectrometer. Mol Cell Proteomics MCP. 2018;17:2534–45.
32. Tran NH, Qiao R, Xin L, Chen X, Liu C, Zhang X, et al. Deep learning enables de novo peptide sequencing from data-independent-acquisition mass spectrometry. Nat Methods. 2019;16:63–6.
33. Soul J, Hardingham TE, Boot-Handford RP, Schwartz J-M. SkeletalVis: an exploration and meta-analysis data portal of cross-species skeletal transcriptomics data. Bioinformatics. 2019;35:2283–90.
34. Soul J, Barter MJ, Little CB, Young DA. OATargets: a knowledge base of genes associated with osteoarthritis joint damage in animals. Ann Rheum Dis. 2021;80:376–83.
35. Allas L, Rochoux Q, Leclercq S, Boumédiene K, Baugé C. Development of a simple osteoarthritis model useful to predict in vitro the anti-hypertrophic action of drugs. Lab Investig J Tech Methods Pathol. 2020;100:64–71.
36. Aury-Landas J, Bazille C, Allas L, Bouhout S, Chesneau C, Leclercq S, et al. Anti-inflammatory and chondroprotective effects of the S-adenosylhomocysteine hydrolase inhibitor 3-Deazaneplanocin a, in human articular chondrocytes. Sci Rep. 2017;7:6483.
37. Lorenz W, Buhrmann C, Mobasheri A, Lueders C, Shakibaei M. Bacterial lipopolysaccharides form procollagen-endotoxin complexes that trigger cartilage inflammation and degeneration: implications for the development of rheumatoid arthritis. Arthritis Res Ther. 2013;15:R111.
38. Caccese RG, Zimmerman JL, Carlson RP. Bacterial lipopolysaccharide potentiates type II collagen-induced arthritis in mice. Mediat Inflamm. 1992;1:273–9.
39. Huang ZY, Stabler T, Pei FX, Kraus VB. Both systemic and local lipopolysaccharide (LPS) burden are associated with knee OA severity and inflammation. Osteoarthr Cartil. 2016;24:1769–75.
40. Mendez ME, Sebastian A, Murugesh DK, Hum NR, McCool JL, Hsia AW, et al. LPS-induced inflammation prior to injury exacerbates the development of post-traumatic osteoarthritis in mice. J Bone Miner Res Off J Am Soc Bone Miner Res. 2020;35:2229–41.
41. Park S, Lee LR, Seo JH, Kang S. Curcumin and tetrahydrocurcumin both prevent osteoarthritis symptoms and decrease the expressions of pro-inflammatory cytokines in estrogen-deficient rats. Genes Nutr. 2016;11:2.
42. Yang Q, Wu S, Mao X, Wang W, Tai H. Inhibition effect of curcumin on TNF-α and MMP-13 expression induced by advanced glycation end products in chondrocytes. Pharmacology. 2013;91:77–85.
43. Kumar D, Kumar M, Saravanan C, Singh SK. Curcumin: a potential candidate for matrix metalloproteinase inhibitors. Expert Opin Ther Targets. 2012;16:959–72.
44. Zhao P, Cheng J, Geng J, Yang M, Zhang Y, Zhang Q, et al. Curcumin protects rabbit articular chondrocytes against sodium nitroprusside-induced apoptosis in vitro. Eur J Pharmacol. 2018;828:146–53.
45. Dragos D, Gilca M, Gaman L, Vlad A, Iosif L, Stoian I, et al. Phytomedicine in joint disorders. Nutrients. 2017;9.
46. Gagnier JJ, Chrubasik S, Manheimer E. Harpgophytum procumbens for osteoarthritis and low back pain: a systematic review. BMC Complement Altern Med. 2004;4:13.
47. Lim DW, Kim JG, Han D, Kim YT. Analgesic effect of Harpagophytum procumbens on postoperative and neuropathic pain in rats. Mol Basel Switz. 2014;19:1060–8.
48. Brien S, Lewith G, Walker A, Hicks SM, Middleton D. Bromelain as a treatment for osteoarthritis: a review of clinical studies. Evid-Based Complement Altern Med ECAM. 2004;1:251–7.
49. Cohen A, Goldman J. Bromelains therapy in rheumatoid arthritis. Pa Med J. 1928;1964(67):27–30.
50. Kumakura S, Yamashita M, Tsurufuji S. Effect of bromelain on kaolin-induced inflammation in rats. Eur J Pharmacol. 1988;150:295–301.


## Publisher's Note